

# Thiaoxaaza-Macrocyclic Chromoionophores as Mercury(II) Sensors: Synthesis and Color Modulation

Hayan Lee and Shim Sung Lee\*

Department of Chemistry (BK21) and Research Institute of Natural Science,  
Gyeongsang National University, Jinju 660-701, South Korea

sslee@gnu.ac.kr

Received February 4, 2009

## ABSTRACT



Azo-coupled macrocyclic chromoionophores incorporating benzene ( $L^1$ ) and pyridine ( $L^2$ ) subunits were synthesized, respectively. In a cation-induced color change experiment, both receptors showed  $Hg^{2+}$  selectivity. However,  $L^1$  gave a larger cation-induced hypsochromic shift than  $L^2$ , suggesting that the presence of the pyridine unit in  $L^2$  may inhibit the  $Hg\cdots N$ -azo interaction. The observed  $Hg^{2+}$ -selective color changes for  $L^1$  and  $L^2$  were found to be controlled by anion-coordination ability. NMR titration of the proposed receptor ligand with  $Hg(II)$  salt was accomplished.

Synthetic receptors for sensing and recognizing environmentally and biologically important ionic species are currently of widespread interest.<sup>1</sup> In this category of sensor molecules, *N*-azo-coupled macrocyclic systems<sup>2</sup> represent a promising research area, not only in terms of their chromophoric function<sup>3</sup> but also because of their high selectivity for the metal species of interest, including heavy metal ions.<sup>4</sup>

Previously, we reported the synthesis of  $NO_2S_2$  macrocycles<sup>5</sup> that show an affinity for  $Hg^{2+}$  and bind to this cation in an exo-<sup>5b,6</sup> or endo-coordination<sup>5b,7</sup> manner. More recently, we synthesized an *N*-azo-coupled analogue that shows  $Hg^{2+}$  selectivity with the color of the  $Hg^{2+}$  complex also controlled by the nature of the anion present. As an extension,

(1) (a) Nolan, E. M.; Lippard, S. J. *Chem. Rev.* **2008**, *108*, 3443. (b) Kim, H. N.; Lee, M. H.; Kim, H. J.; Kim, J. S.; Yoon, J. *Chem. Soc. Rev.* **2008**, 1465. (c) Cheng, T.; Xu, Y.; Zhang, S.; Zhu, W.; Qian, X.; Duan, L. *J. Am. Chem. Soc.* **2008**, *130*, 16160. (d) Yantasee, W.; Warner, C. L.; Sangvanich, T.; Addleman, R. S.; Carter, T. G.; Wiacek, R. J.; Fryxell, G. E.; Timchalk, C.; Warner, M. G. *Environ. Sci. Technol.* **2007**, *41*, 5114. (2) (a) Lee, S. J.; Jung, J. H.; Seo, J.; Yoon, I.; Park, K.-M.; Lindoy, L. F.; Lee, S. S. *Org. Lett.* **2006**, *8*, 1641. (b) Kim, J. S.; Shon, O. J.; Lee, J. K.; Lee, S. H.; Kim, J. Y.; Park, K.-M.; Lee, S. S. *J. Org. Chem.* **2002**, *67*, 1372.

(3) (a) Nishiyabu, R.; Palacios, M. A.; Dehaen, W.; Anzenbacher, P., Jr. *J. Am. Chem. Soc.* **2006**, *128*, 11496. (b) Lee, H. G.; Lee, J.-E.; Choi, K. S. *Inorg. Chem. Commun.* **2006**, *9*, 582. (c) Beer, P. D.; Gale, P. A. *Angew. Chem., Int. Ed.* **2001**, *40*, 486. (d) Lavigne, J. J.; Anslyn, E. V. *Angew. Chem., Int. Ed.* **2001**, *40*, 3118. (e) Izatt, R. M.; Pawlak, K.; Bradshaw, J. S. *Chem. Rev.* **1991**, *91*, 1721. (f) Dix, J. P.; Vögtle, F. *Chem. Ber.* **1981**, *114*, 638. (g) Dix, J. P.; Vögtle, F. *Chem. Ber.* **1980**, *113*, 457.

(4) (a) Lee, S. J.; Bae, D. R.; Han, W. S.; Lee, S. S.; Jung, J. H. *Eur. J. Inorg. Chem.* **2008**, 1559. (b) Kim, J. S.; Quang, D. T. *Chem. Rev.* **2007**, *107*, 3780. (c) Onyido, I.; Norris, A. R.; Buncel, E. *Chem. Rev.* **2004**, *104*, 5911. (d) de Silva, A. P.; Fox, D. B.; Huxley, A. J. M.; Moody, T. S. *Coord. Chem. Rev.* **2000**, *205*, 41. (e) Amendola, V.; Fabbri, L.; Lincchelli, M.; Mangano, C.; Pallavicini, P.; Parodi, L.; Poggi, A. *Coord. Chem. Rev.* **1999**, *190–192*, 649.

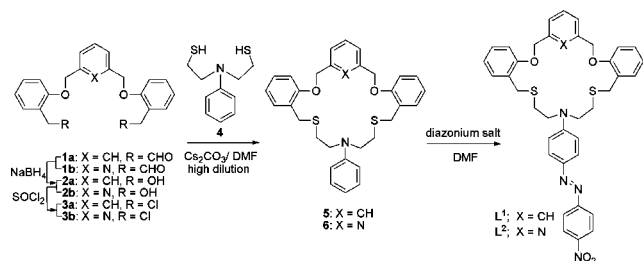
(5) (a) Park, C. S.; Lee, J. Y.; Kang, E.-J.; Lee, J.-E.; Lee, S. S. *Tetrahedron Lett.* **2009**, *50*, 671. (b) Jin, Y.; Yoon, I.; Seo, J.; Lee, J.-E.; Moon, S.-T.; Kim, J.; Han, S. W.; Park, K.-M.; Lindoy, L. F.; Lee, S. S. *Dalton Trans.* **2005**, 788.

(6) (a) Lee, S. Y.; Park, S.; Kim, H. J.; Jung, J. H.; Lee, S. S. *Inorg. Chem.* **2008**, *47*, 1913. (b) Sultana, K. F.; Lee, S. Y.; Lee, J. Y.; Park, K.-M.; Lee, S. S. *Bull. Korean Chem. Soc.* **2008**, *29*, 241. (c) Lee, J.-E.; Jin, Y.; Seo, J.; Yoon, I.; Song, M. R.; Lee, S. Y.; Park, K.-M.; Lee, S. S. *Bull. Korean Chem. Soc.* **2006**, *27*, 203.

(7) (a) Seo, J.; Lee, S. S.; Gong, W.-T.; Hiratani, K. *Tetrahedron Lett.* **2008**, *49*, 3770. (b) Choi, K. S.; Kang, D.; Lee, J.-E.; Seo, J.; Lee, S. S. *Bull. Korean Chem. Soc.* **2006**, *27*, 747.

we are currently working on the synthesis of new macrocyclic chromoionophores for the selective detection of heavy metal ions and have undertaken a comparative structure–function analysis of metal sensing by the *N*-azo-coupled macrocycles incorporating benzene (**L**<sup>1</sup>) and pyridine (**L**<sup>2</sup>) subunits as part of their macrocyclic backbones (Scheme 1). We herein report the synthesis of **L**<sup>1</sup> and **L**<sup>2</sup> as an investigation of their structure–function relationship, with emphasis on the color-modulation in metal ion sensing.

**Scheme 1.** Synthesis of Azo-Coupled Macrocycles



As key precursors, *N*-phenylated macrocycles **5** and **6** were synthesized by dithiol–dichloride coupling reactions of **4** with **3a** or **3b**, employing Cs<sub>2</sub>CO<sub>3</sub> under high dilution. **L**<sup>1</sup> and **L**<sup>2</sup> were synthesized by the reactions of the diazonium salt of *p*-nitroaniline with **5** and **6**, respectively. Red single crystals of **L**<sup>2</sup> were obtained by vapor diffusion of *n*-hexane into dichloromethane solution, and the crystal structure of this product was obtained (Figure 1). In **L**<sup>2</sup>, the macrocyclic ring is flattened with the two torsion angles between the S and N donors indicating a propensity for each linkage to adopt an anti-anti conformation.

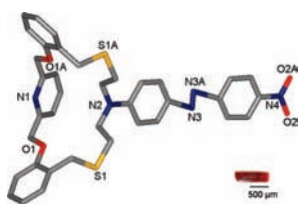


**Figure 1.** Crystal structure of **L**<sup>2</sup>.

The metal-binding properties of **L**<sup>1</sup> and **L**<sup>2</sup> were examined by UV–vis spectrophotometry with respect to the induced color changes (Figure 2). **L**<sup>1</sup> and **L**<sup>2</sup> both exhibit intense absorptions at 480 nm (red,  $\epsilon_{\text{max}}$ : 27300 for **L**<sup>1</sup> and 23300 for **L**<sup>2</sup>). Notably, the addition of Hg<sup>2+</sup> resulted in the largest hypsochromic shift: to 339 nm for **L**<sup>1</sup> ( $\Delta\lambda$  = 142 nm) and 378 nm for **L**<sup>2</sup> ( $\Delta\lambda$  = 102 nm), changing their solution colors from red to colorless and pale-yellow, respectively (Figure 2). In contrast, no significant color changes were observed upon addition of other metal ions, except Cu<sup>2+</sup> for **L**<sup>1</sup> and Ag<sup>+</sup> for **L**<sup>2</sup> (Figure 2).

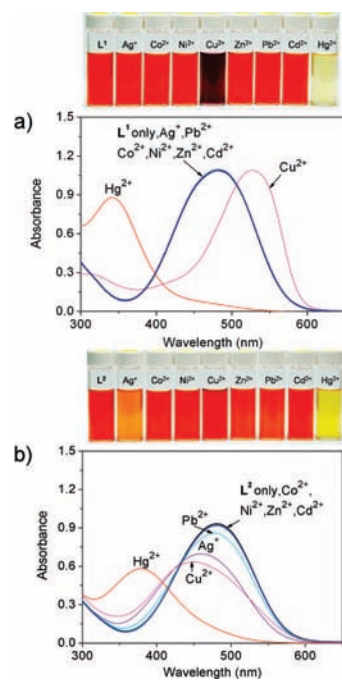


**Figure 2.** UV/vis spectra of (a) **L**<sup>1</sup> and (b) **L**<sup>2</sup> (40  $\mu$ M) in the presence of metal perchlorates (5.0 equiv) in acetonitrile.

The titrations of **L**<sup>1</sup> and **L**<sup>2</sup> with Hg(ClO<sub>4</sub>)<sub>2</sub> resulted in the absorption at 480 nm gradually decreasing whereas the absorptions at 378 and 339 nm gradually increased to give isosbestic points at 415 and 399 nm (Figure 3b), respectively.

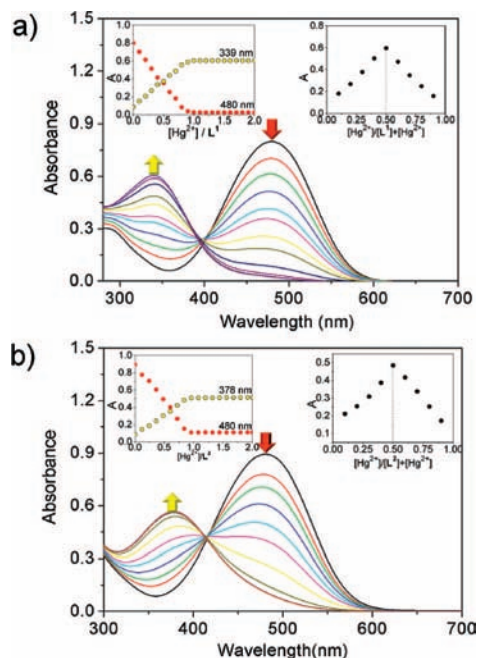


**Figure 3.** Spectrophotometric titrations of (a) **L**<sup>1</sup> and (b) **L**<sup>2</sup> (40  $\mu$ M) with Hg(ClO<sub>4</sub>)<sub>2</sub> in acetonitrile. Inset: (left) titration curves and (right) Job plots.

In both cases, a 1:1 (L/M) stoichiometry for complexation was evident from each titration curve and also from Job plots for each system. The titration plots were very sharp, and hence, the stability constants are too high to be calculated using this data in least-squares nonlinear fitting programs.

In  $\text{Hg}^{2+}$  selectivity measurements, the absorbance of the  $\text{Hg}^{2+}$ – $\text{L}^1$  complex was not affected in the presence of 10 equiv of other competing metal ions such as  $\text{Ag}^+$ ,  $\text{Co}^{2+}$ ,  $\text{Ni}^{2+}$ ,  $\text{Cu}^{2+}$ ,  $\text{Zn}^{2+}$ ,  $\text{Pb}^{2+}$ ,  $\text{Cd}^{2+}$ ,  $\text{Li}^+$ ,  $\text{K}^+$ ,  $\text{Ca}^{2+}$ , and  $\text{Mg}^{2+}$  (Figure S10, Supporting Information). These results are different from those obtained with other  $\text{Hg}^{2+}$  sensor molecules that have usually also been affected by  $\text{Ag}^+$  and other heavy metal ions.<sup>4</sup> However, in contrast, the absorbance of the  $\text{Hg}^{2+}$ – $\text{L}^2$  complex showed a 10–15% decrease when  $\text{Ag}^+$ ,  $\text{Co}^{2+}$ ,  $\text{Ni}^{2+}$ , and  $\text{Cd}^{2+}$  were added to the solution.

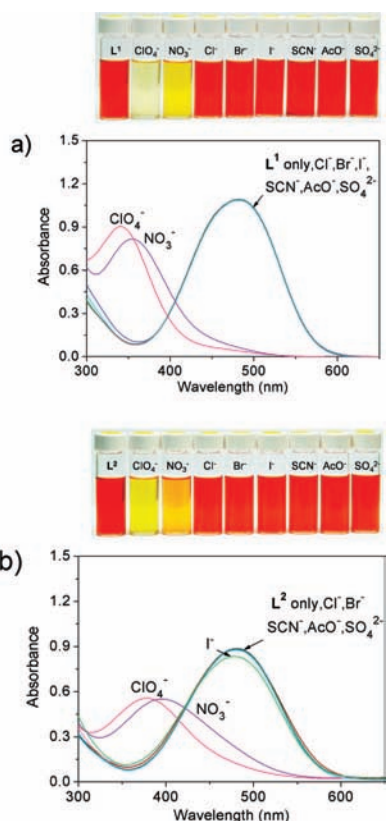


**Figure 4.** UV/vis spectra of (a)  $\text{L}^1$  and (b)  $\text{L}^2$  (40  $\mu\text{M}$ ) in the presence of  $\text{Hg}^{2+}$  salts (5.0 equiv) in acetonitrile.

We also found that the color change with  $\text{Hg}^{2+}$  may vary with the anion present. For instance, the addition of  $\text{ClO}_4^-$  or  $\text{NO}_3^-$  resulted in hypochromic shifts to 367 and 350 nm (pale yellow), respectively (Figure 4). However, no color change was observed upon addition of  $\text{Cl}^-$ ,  $\text{Br}^-$ ,  $\text{I}^-$ ,  $\text{AcO}^-$ ,  $\text{SCN}^-$ , or  $\text{SO}_4^{2-}$ . This is attributed to the significant coordinating ability of these latter anions to the  $\text{Hg}^{2+}$  ion.<sup>2a</sup> The results indicate that **1** not only can be useful as an efficient chromogenic reagent for cation sensing but also shows promise as a reagent for  $\text{ClO}_4^-$  and  $\text{NO}_3^-$  sensing in the presence of a range of other anions. The observed behavior undoubtedly reflects the structures of the

respective complexes generated, and thus, we decided to attempt the preparation and crystal structure of each of the colored species.

We were successful in isolating yellow-red (**1**) and red (**2**) complexes as single crystals from solutions of  $\text{L}^2$  with  $\text{Hg}(\text{ClO}_4)_2$  and  $\text{Hg}(\text{NO}_3)_2$ , respectively, and their structures were obtained by X-ray diffraction (Figure 5). The X-ray analysis revealed that **1** is a 1:1 complex of type  $[\text{Hg}(\text{L}^2)](\text{ClO}_4)_2(\text{DMF})$  (Figure 5a). The Hg atom is located at the center of  $\text{L}^2$  which adopts a bent arrangement. Hg1 is five-coordinate, being bound to two S, two O and one pyridine N atom. An intramolecular  $\pi\cdots\pi$  stacking interaction (3.29 Å and 16.7°, dashed line in Figure 5a) occurs between two aromatic groups.

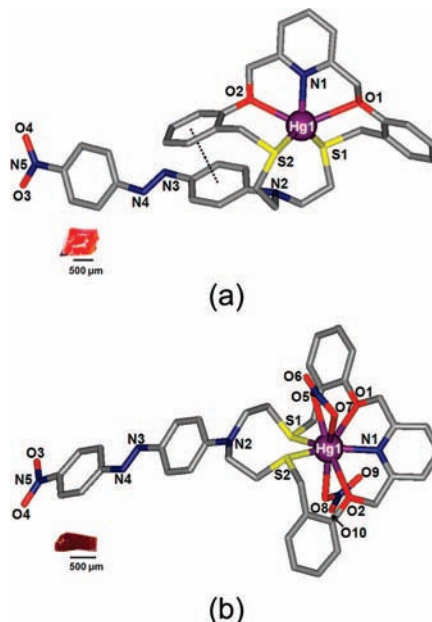


**Figure 5.** Crystal structures of  $\text{L}^2$  complexes with  $\text{Hg}^{2+}$  salts: (a) **1**,  $[\text{Hg}(\text{L}^2)](\text{ClO}_4)_2(\text{DMF})$  and (b) **2**,  $[\text{Hg}(\text{L}^2)](\text{NO}_3)_2$ . Noncoordinated anions and solvent molecule are omitted.

On reaction with  $\text{Hg}(\text{NO}_3)_2$ ,  $\text{L}^2$  forms the 1:1 endotype complex  $[\text{Hg}(\text{L}^2)](\text{NO}_3)_2$  (**2**). Unlike **1**, this dinitrato complex is a neutral species; the Hg center in the cavity is coordinated to an  $\text{NS}_2\text{O}_2$  donor set from the macrocycle (but not to the *t*-N atom) as well as to two nitrate ions bound in a mono- and a bidentate manner. Considering the narrow bite angle [ $\text{O5}–\text{Hg1}–\text{O7}$  44.94(3)°] of the bidentate nitrate ion, the geometry of the Hg coordination sphere is probably best described as pseudopentagonal bipyramidal. The  $\text{NS}_2\text{O}_2$  donors of  $\text{L}^2$  define the equatorial plane, with the axial positions occupied by the two nitrate ligands.

In both complexes of  $\text{L}^2$ , the distances between Hg and the *t*-N atom (3.290 Å for **1** and 4.478 Å for **2**) are too long to be considered as a regular bond,<sup>8</sup> with the longer distance in **2** than that in **1** being attributed to the presence of anion coordination. Consequently, it is the presence of the pyridine unit in  $\text{L}^2$  that may inhibit bond formation between Hg and the

*t*-N atom and results in this dye receptor being less sensitive than **L**<sup>1</sup> as exemplified by the results presented in Figures 2 and 3 (see also Figure S11, Supporting Information).

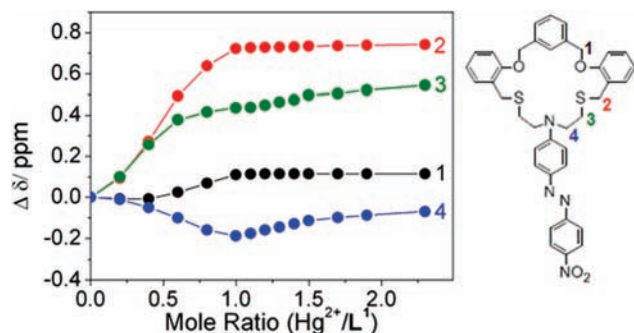


**Figure 6.** <sup>1</sup>H NMR titration curves for **L**<sup>1</sup> with Hg(ClO<sub>4</sub>)<sub>2</sub> in CDCl<sub>3</sub>/CD<sub>3</sub>CN (v/v 1:6).

Unfortunately, single crystals of the corresponding Hg<sup>2+</sup> complexes of **L**<sup>1</sup> were not able to be obtained. Instead, the binding behavior of **L**<sup>1</sup> toward Hg<sup>2+</sup> was further investigated by NMR titration (Figure 6). The signals of the methylene protons (H<sub>1–4</sub>) in **L**<sup>1</sup> (Figure S9a) were well resolved. Upon addition of Hg(ClO<sub>4</sub>)<sub>2</sub> to a solution of **L**<sup>1</sup>, all of the protons display downfield shifts except for H<sub>4</sub>, in keeping with **L**<sup>1</sup> forming a stable complex with Hg<sup>2+</sup>, which shows a fast-exchange rate between ligand and cation on the NMR time scale. The titration curves [plotting Δδ (ppm) vs added equiv of Hg<sup>2+</sup>] for each proton clearly show an inflection point at a mole ratio (Hg/L) of 1.0, indicating a 1:1 solution stoichiometry for the complex. The order of magnitude of the chemical shift variation for the aliphatic region is H<sub>2</sub> (Δδ: 0.74 ppm) > H<sub>3</sub> (0.54 ppm) > H<sub>4</sub> (0.19 ppm) > H<sub>1</sub> (0.11 ppm). The larger chemical shift changes shown by the H<sub>2</sub>, H<sub>3</sub>, and H<sub>4</sub> adjacent to the S and N atoms can be explained by the likelihood that the Hg<sup>2+</sup> is strongly bound to the S and N donors, while the O donors interact with the Hg<sup>2+</sup> relatively weakly.

The 1:1 (Hg/L) stoichiometry of the Hg<sup>2+</sup> complexes with each ligand is also confirmed by their fast atom bombardment

(FAB) mass spectra, which show peaks corresponding to [Hg(**L**<sup>1</sup>)ClO<sub>4</sub>]<sup>+</sup> (*m/z* 977.2) and [Hg(**L**<sup>2</sup>)ClO<sub>4</sub>]<sup>+</sup> (*m/z* 978.2), respectively (Figure 7). The relative abundance of their isotope peak patterns are in each case in good agreement with the corresponding simulated peak patterns.

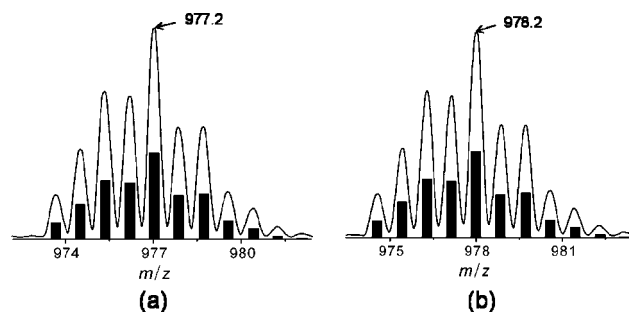


**Figure 7.** Observed isotope distributions for (a) [Hg(**L**<sup>1</sup>)ClO<sub>4</sub>]<sup>+</sup> and (b) [Hg(**L**<sup>2</sup>)ClO<sub>4</sub>]<sup>+</sup> in the FAB mass spectra of Hg(ClO<sub>4</sub>)<sub>2</sub> complexes of **L**<sup>1</sup> and **L**<sup>2</sup>, respectively. The bars represent the predicted mass spectral distributions for these ions.

In summary, the synthesis and comparative chromogenic behavior of the *N*-azo-coupled thiaoxaaza-macrocycles incorporating benzene (**L**<sup>1</sup>) and pyridine (**L**<sup>2</sup>) subunits are presented. **L**<sup>1</sup> exhibits better Hg<sup>2+</sup> selectivity and sensitivity than **L**<sup>2</sup> because of the coordination of the pyridine nitrogen in **L**<sup>2</sup> inhibiting the bond formation between Hg<sup>2+</sup> and the macrocyclic *t*-N atom, with the observed induced color being very sensitive to this effect. This result may contribute not only to the design and synthesis of new chromoionophores for the selective detection of heavy metal ions but also in the development of related nanosensing materials based on the structure–function analysis.

**Acknowledgment.** This work was supported by KOSEF (Grant No. R01-2007-000-20245-0). The authors thank Prof. L. F. Lindoy for his advice.

**Supporting Information Available:** Syntheses of **L**<sup>2</sup>, **1** and **2**; X-ray crystallographic files (CIF); NMR data. This material is available free of charge via the Internet at <http://pubs.acs.org>.

OL900241P

(8) (a) Hancock, R. D.; Reibenspies, J. H.; Maumela, H. *Inorg. Chem.* **2004**, *43*, 2981. (b) Hossain, G. M. G.; Amoroso, A. J.; Banu, A.; Malik, K. M. A. *Polyhedron* **2007**, *26*, 967. (c) Gupta, P. K. S.; Houk, L. W.; van der Helm, D.; Hossain, M. B. *Inorg. Chim. Acta* **1980**, *44*, L235. (d) Bebout, D. C.; Bush, J. F.; Crahan, K. K.; Bowers, E. V.; Butcher, R. J. *Inorg. Chem.* **2002**, *41*, 2529.